condensed matter

MDPI

Article

Pump-Probe X-ray Photoemission Spectroscopy of Free-Standing Graphane

Roberto Costantini [1,2,*], Dario Marchiani [3], Maria Grazia Betti [3], Carlo Mariani [3,4,*], Samuel Jeong [5], Yoshikazu Ito [5], Alberto Morgante [1,2] and Martina Dell'Angela [2,*]

1 Dipartimento di Fisica, Università di Trieste, Via Valerio 2, I-34127 Trieste, Italy
2 Istituto Officina dei Materiali CNR-IOM, Strada Statale 14–km 163.5, I-34149 Trieste, Italy
3 Dipartimento di Fisica, Università di Roma "La Sapienza", P.le Aldo Moro 2, I-00185 Roma, Italy
4 INFN Sezione di Roma, P.le Aldo Moro 2, I-00185 Roma, Italy
5 Institute of Applied Physics, Graduate School of Pure and Applied Sciences, University of Tsukuba, Tsukuba 305-8573, Japan
* Correspondence: costantini@iom.cnr.it (R.C.); carlo.mariani@uniroma1.it (C.M.); dellangela@iom.cnr.it (M.D.)

Abstract: Free-standing nanoporous graphene was hydrogenated at about 60 at.% H uptake, as determined by the emerging of the sp^3 bonding component in the C 1s core level investigated by high-resolution X-ray photoelectron spectroscopy (XPS). Fully unsupported graphane was investigated by XPS under optical excitation at 2.4 eV. At a laser fluence of 1.6 mJ/cm^2, a partial irreversible dehydrogenation of the graphane was observed, which could be attributed either to the local temperature increase or to a photo-induced softening of the H-to-C stretching mode. The sub-ns dynamics of the energy shift and peak broadening of the C 1s core level revealed two different decay constants: 210 ps and 130 ps, respectively, the former associated with photovoltage dynamics and the latter with thermal heating on a time scale comparable with the synchrotron temporal resolution.

Keywords: nanoporous graphene; graphane; pump-probe spectroscopy; time-resolved spectroscopy; X-ray photoelectron spectroscopy

Citation: Costantini, R.; Marchiani, D.; Betti, M.G.; Mariani, C.; Jeong, S.; Ito, Y.; Morgante, A.; Dell'Angela, M. Pump-Probe X-ray Photoemission Spectroscopy of Free-Standing Graphane. *Condens. Matter* **2023**, *8*, 31. https://doi.org/10.3390/condmat8020031

Academic Editors: Augusto Marcelli, Massimo Ferrario, Marcello Coreno and Francesco Stellato

Received: 15 February 2023
Revised: 17 March 2023
Accepted: 24 March 2023
Published: 27 March 2023

1. Introduction

The functionalization of graphene (Gr) with atomic hydrogen has been predicted to lead to a two-dimensional (2D) semiconducting carbon sheet, obtaining graphane [1,2]. In such a material, H binds with C atoms, modifying the pristine planar sp^2 to a sp^3 deformed hybridization [1,2]. A variety of methods have been used so far to produce graphane by chemisorbing atomic hydrogen or deuterium, from plasma [3–7] to temperature-induced molecular cracking [8,9], on exfoliated or substrate-supported Gr [4,6,8–14].

Only recently high-quality and stable graphane has been produced as fully unsupported and free-standing [15–18], by using nanoporous graphene (NPG) [19–23] as substrate, with ultra-high-vacuum high-temperature molecular cracking as the atomic H source [18]. In particular, the gap-opening and the sp^3 bond formation of graphane have been observed by high resolution UV and X-ray photoelectron spectroscopy [18].

Graphane has been recently proposed as scaffold for tritium atom grafting in a futuristic neutrino detector [24]; therefore, the dynamics and the stability of the sp^3 chemical bond studied by using its lighter isotopes constitute fundamental issues to be assessed before any application. On the other hand, while the photoinduced dynamics of graphene have been thoroughly studied in the last decade [25–27], the dynamics of graphane are still experimentally unknown. Thanks to the achievement of fully free-standing NPG-based graphane, we have the opportunity to investigate its dynamics without any interference from substrates and/or defects. In fact, nanoporous graphene alone can foster a conversion to graphane with a high density of C−ligible presence H bonds, and a finely monitored in

situ hydrogenation in ultra-high vacuum conditions on such a template leads to a negof unsaturated bonds or defects [18]. In the following paragraphs, we study the sub-nanosecond temporal evolution of the C 1s core level by X-ray photoelectron spectroscopy (XPS) after exciting the H-NPG sample with femtosecond optical pulses (2.4 eV). The ~100 ps temporal resolution achievable at synchrotron facilities provides important information concerning the sample stability and its damage threshold, which must be determined prior to any time-resolved experiment. We show that a pump fluence of 1.6 mJ/cm^2 causes a partial dehydrogenation of graphane, which we tentatively assign to the local laser-induced heating. On the sub-nanosecond range, we observe the transient broadening and shift of the C 1s core level with two different time constants, which we ascribed to lattice heating and surface photovoltage, respectively.

2. Results and Discussion

The C 1s core level line shape is an excellent fingerprint of the chemical bonding of carbon. Hydrogen (or deuterium) chemisorption on Gr produces a neat sp^3 component at higher binding energy (BE) with respect to the Gr component related to the planar sp^2 hybridized bonds [15–18].

The C 1s core-level for a high-coverage H-NPG sample probed with 400 eV photon energy is shown in Figure 1a. We used Doniach–Sunjic line shapes to fit the data, with the best fitting of the spectrum presenting dominant sp^2 and sp^3 components and a minor CO_x one due to residual contamination at 284.5 eV, 285.0 eV, and 285.8 eV BE, respectively. Defining the intensity ratio $\Theta = sp^3/(sp^2 + sp^3)$ allows to estimate the hydrogen uptake, which is about 60 at.%. The H-NPG sample was successively illuminated with a pulsed laser (128 kHz repetition rate) at 2.4 eV photon energy and a 1.6 mJ/cm^2 fluence, revealing an evident C 1s line shape change (Figure 1b), corresponding to an irreversible decrease in Θ to ~20 at.%, thus compatible to a reduction of the H content. The reduction of Θ shown in Figure 1b occured immediately after exposure of the sample to laser radiation and remained unaltered for longer exposure times at the same fluence.

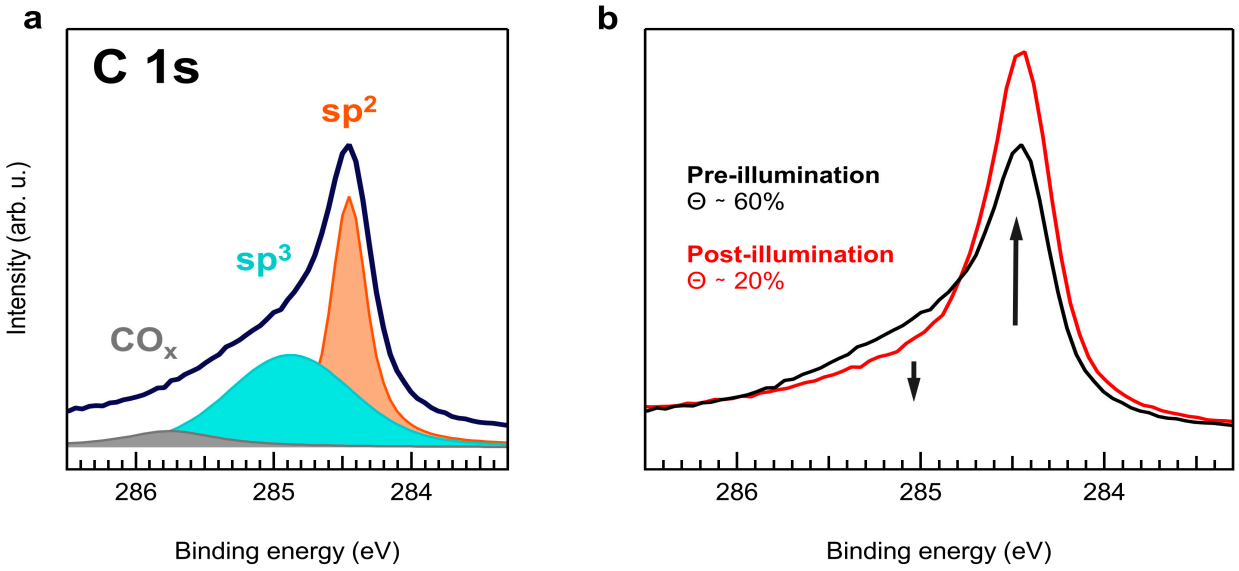

Figure 1. C 1s XPS spectra of H-NPG measured with 400 eV photon energy. (**a**) Spectrum of the pristine sample (black) and fitting components: sp^2 (orange), sp^3 (blue), and CO_x (gray). (**b**) C 1s XPS data before (black) and after (red) illumination with 2.4 eV photons at 1.6 mJ/cm^2 fluence. The two arrows mark the opposite intensity behavior of the sp^2 and sp^3 components after laser illumination.

Hydrogen desorption might be ascribed to different causes, such as the local laser-induced heating or an electronically initiated dehydrogenation. We can first infer the

base temperature increase under the ΔT_{CW} laser approximation by using heat diffusion models [28]:

$$\Delta T_{CW} \approx \frac{P\,(1-R_c)}{2\sqrt{\pi}\,k\,w} \quad (1)$$

with P representing the laser power, R_c the reflection coefficient, k the thermal diffusivity of the material, and $w = 150$ µm the beam radius in this experiment. The temperature increase depends on the estimated parameters of graphane (absorbance, thermal diffusivity). Considering an absorbance $(1 - R_c)$ of 2.3% [29] and a thermal diffusivity of the order of ~10 W/(m K) [30,31], (1) gives a temperature increase in the range of few K.

The maximum temperature reached before dissipation depends on the laser pulse energy, heat capacity, and mass density instead [28]:

$$\Delta T_{Max} = \frac{Q\,(1-R_c)}{\pi\,w^2\,d\,C_p\,\rho_m} \quad (2)$$

with Q representing the pulse energy, d the absorption depth, C_p the heat capacity, and ρ_m the mass density. Assuming $d = 3 \times 10^{-8}$ m [32], and using the predicted heat capacity of graphane 15% larger than that of Gr [33], C_p ~800 J/(Kg K), and the much lower expected mass density of NPG in the range of from 3 to 70 kg/m^3 [34], the maximum T reached locally under the laser pulse can be of several hundreds of K, close to the 920 K required to recover pristine Gr with total desorption of H atoms [15]. However, these evaluations are largely based on partially known parameters (mass density, heat capacity, thermal diffusivity, absorbance), often only predicted for graphane since free-standing and fully hydrogenated graphane is very difficult to be synthesized. Thus, we cannot exclude a preferential electronically induced dehydrogenation, associated with the laser-induced softening of the C-H stretching as predicted by first-principles simulations based on time-dependent density functional theory [35], although the fluence used in the calculations was one order of magnitude higher.

We proceeded to study the photo-induced dynamics of the C 1s core level by time-resolved XPS in the sub-ns time scale. Laser pulses of 2.4 eV at a 1.6 mJ/cm^2 fluence were used to excite the sample, while 400 eV synchrotron pulses were used as a probe. As reported in Figure 1, laser exposure at this fluence immediately resulted in a partial dehydrogenation to Θ ~20 at.%; successively, the sample stability under constant illumination was ensured by the overlap between the first and last spectra of the time-resolved sequence, acquired almost two hours apart. The high energy resolution and high brilliance of synchrotron radiation allow to discriminate C-to-H sp^3 and C-to-C sp^2 components in the measured C 1s spectra, albeit with a limited temporal resolution imposed by the synchrotron pulse duration (~100 ps). In Figure 2, the broadening and binding energy shift of sp^2 (orange) and sp^3 (blue) components is shown as a function of the pump-probe delay.

We observed a spectral shift to lower binding energies (−0.1 eV) accompanied by a significant broadening (~0.3 eV) of both components. We fitted the relaxation dynamics by using exponentially modified Gaussian distributions (solid lines), with the Gaussian full width at half maximum (FWHM) constrained to 120 ps, to account for the pump-probe cross-correlation. The fits yield two different time constants, namely $\tau_B = 130 \pm 20$ ps for the broadening and $\tau_S = 210 \pm 10$ ps for the shift, with the distinct decay rates suggesting that the two effects may be characterized by a different nature. With respect to the broadening, the ultrafast dynamics of the C 1s line of graphene have been studied at a free electron laser, showing that the electronic temperature decays on a much faster time scale [36], therefore suggesting that the lattice heating is a more likely cause of the change in the C 1s width in our data. Under this assumption, if we relate the ~0.3 eV broadening at time zero to the temperature-dependent phonon broadening measured in graphene [37], we find that the instantaneous temperature increase is of more than 1000 K, thus again suggesting that the dehydrogenation might be thermally induced.

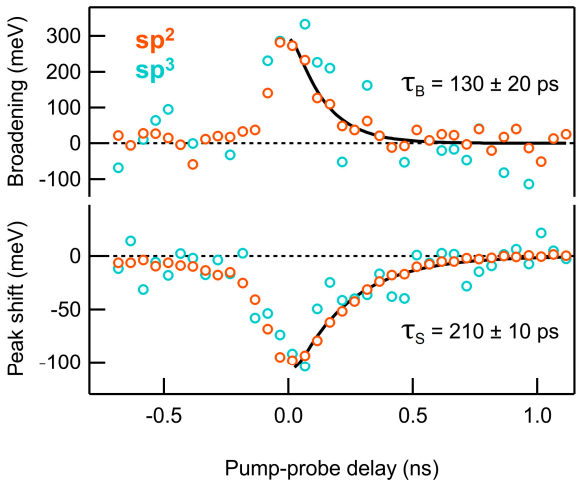

Figure 2. Broadening and binding energy shift of sp^2 (orange) and sp^3 (blue) components as extracted from the fits of C 1s photoemission lines; exponentially modified Gaussian distributions (solid curves) are used to fit the broadening and shift relaxation dynamics. The scattering of the data points reflects the uncertainty in the results obtained from the fits of the C 1s spectra.

With respect to the energy shift, we identify three possible causes: local heating, surface photovoltage (SPV), and space charge effects. It is known that the temperature increase may cause core level shifts in metals [38] and graphene [37] due to the lattice expansion, but the differences in the dynamics of the observed broadening and shift do not support such a hypothesis. The shift is more likely ascribed to the transient surface photovoltage (SPV) field, which is related to the semiconducting character of H-NPG [18] and arises as a result of the separation of the photo-generated excitons. Space charge effects may also induce a similar shift, but they depend on the number of electrons photoemitted by the pump pulse. Since the pump photon energy is well below the direct gap of graphane, the laser-induced photoemission is low in our measurement, thus suggesting that space charge effects are negligible compared to SPV.

To conclude, we note that the decay times obtained from our data are close to the temporal resolution of the synchrotron. Moreover, the measured relaxation of sp^3 and sp^2 broadening and shift are in perfect overlap, thus revealing no distinction between the two chemically inequivalent species in the 100 ps range. To achieve a deeper understanding of the photo-induced dynamics in H-NPG, and possibly to detect a difference in the response to optical excitations in C-to-H and C-to-C atoms, it would be beneficial to measure time-resolved XPS on such a system at free electron lasers, exploiting the shorter pulse duration to access the sub-picosecond time scale.

3. Materials and Methods

Nanoporous graphene was synthesized starting from a nanoporous Ni template that was obtained from a Ni30Mn70 alloy, chemically treated with 0.5 M ammonium sulfate, eventually obtaining the nanoporous Ni substrate. The nanoporous substrate was exposed to benzene vapors in a chemical vapor deposition (CVD) process and annealed at 900 °C for 5 min, thus obtaining Ni-supported NPG. Free-standing NPG was eventually achieved by chemical dissolution of the Ni template by 1.0 M hydrochloric acid. All steps and details of the synthesis and preparation processes and procedures are presented in previous works [19,23,39–42]. Before exposing NPG to the atomic hydrogen in UHV, it was annealed at about 620 °C for several hours, so as to remove residual contamination [16].

Hydrogenation of NPG was performed in UHV using a hydrogen cracker (Focus GmbH), the latter consisting of a capillary with gas inlet for letting H_2 flow into it. The capillary is heated by electron bombardment so as to obtain a highly efficient (more than 95% [43]) cracking into H atoms, which are directed to the NPG sample. The sample was exposed to a total amount (as measured by the UHV ion-gauge) of 3600 L, with

1 L = 1.33 × 10^{-6} mbar s, using a pressure of 1.0 × 10^{-6} mbar. Such exposure resulted in an average uptake of ~60 at.% of H:C (estimated as the $\Theta = sp^3/(sp^3 + sp^2)$ intensity ratio), so as to allow discernment of both sp^2 and sp^3 components in the XPS C 1s spectrum. An on-campus XPS system equipped with a Mg Kα photon source (PSP TA10) and a hemispherical VG Microtech Clam-2 electron analyzer in constant pass energy mode set at 50 eV and with overall energy resolution of $\leq$1 eV was used for a preliminary characterization of the sample.

The H-NPG sample was dry transferred to the ANCHOR-SUNDYN endstation [44] at the ALOISA beamline at the Elettra synchrotron (Italy). We recently demonstrated that such a hydrogenation method is very stable and unaffected by air transport among different laboratories [16]. A mild annealing up to 150 °C was done once mounted in the new UHV chamber, to facilitate desorption of adventitious contamination without affecting the H-C bonds.

In order to define the optimal conditions for the time-resolved measurements, fluence dependent XPS spectra were acquired with the laser and synchrotron beams impinging on the sample at normal incidence in a quasi-collinear geometry, and the photoemission signal was acquired using multibunch radiation. This acquisition method shows both the irreversible modifications of the line shapes due to laser irradiation and the long-lived photo-induced effects averaged in the time elapsed between consecutive laser pulses [45] which is ~8 µs in these measurements (128 kHz repetition rate). The laser was focused to a spot diameter of ~300 µm, slightly larger than the synchrotron beam on the sample surface. Time-resolved XPS measurements were instead acquired using the hybrid mode filling of Elettra, detecting the signal coming only from the isolated pulses as detailed in Ref. [46]. The temporal overlap between pump and probe pulses was calibrated by measuring the SPV shift on a Si crystal, and the delay was scanned with an electronic phase shifter. A pump fluence of 1.6 mJ/cm^2 was chosen for the time-resolved data with the aim of maximizing the transient photo-induced effect while maintaining a sizable and stable hydrogen content.

4. Conclusions

A highly hydrogenated (~60% at.%) fully free-standing and unsupported nanoporous graphene sample was studied using high-resolution XPS under laser excitation at 2.4 eV. The presence of an sp^3 bonding component, resulting from the establishment of H-to-C chemisorption bonds, indicates the achievement of free-standing graphane. Partial dehydrogenation was obtained by illuminating the sample at a laser fluence of 1.6 mJ/cm^2, probably due to local and instantaneous temperature increase. Longer exposure times at the same fluence did not further reduce the hydrogen content. This "static" characterization illustrates the damage threshold and stability of highly hydrogenated graphene under optical excitation, thus defining the experimental constraints for future time-resolved measurements. The photo-induced dynamics in the sub-ns range of the two C 1 components suggests a different time constant for the observed line broadening and energy shift: 130 ps and 210 ps, respectively. In this preliminary study, we tentatively ascribe the two effects to lattice heating (broadening) and surface photovoltage (shift); however, we note that usage of shorter X-ray pulses, available at free electron lasers, would be required in order to disentangle the very origin of the observed response of free-standing graphane to optical excitations.

Author Contributions: Conceptualization, R.C., M.G.B., C.M. and M.D.; investigation, R.C., D.M., A.M. and M.D.; methodology, R.C., D.M. and M.D.; resources, D.M., S.J. and Y.I.; writing—original draft, R.C., C.M. and M.D. All authors have read and agreed to the published version of the manuscript.

Funding: This research was partially funded by PRIN FERMAT (2017KFY7XF) from Italian Ministry MUR, by Sapienza Ateneo funds, and by JSPS KAKENHI (Grant Numbers JP21H02037, JP20H04628).

Data Availability Statement: Data supporting reported results are available by the authors on request.

Acknowledgments: We acknowledge the experimental support by Alessio Giampietri.

Conflicts of Interest: The authors declare no conflict of interest.

References

1. Sofo, J.O.; Chaudhari, A.S.; Barber, G.D. Graphane: A Two-Dimensional Hydrocarbon. *Phys. Rev. B* **2007**, *75*, 153401. [CrossRef]
2. Cudazzo, P.; Attaccalite, C.; Tokatly, I.V.; Rubio, A. Strong Charge-Transfer Excitonic Effects and the Bose-Einstein Exciton Condensate in Graphane. *Phys. Rev. Lett.* **2010**, *104*, 226804. [CrossRef]
3. Elias, D.C.; Nair, R.R.; Mohiuddin, T.M.G.; Morozov, S.V.; Blake, P.; Halsall, M.P.; Ferrari, A.C.; Boukhvalov, D.W.; Katsnelson, M.I.; Geim, A.K.; et al. Control of Graphene's Properties by Reversible Hydrogenation: Evidence for Graphane. *Science (1979)* **2009**, *323*, 610–613. [CrossRef] [PubMed]
4. Luo, Z.; Shang, J.; Lim, S.; Li, D.; Xiong, Q.; Shen, Z.; Lin, J.; Yu, T. Modulating the Electronic Structures of Graphene by Controllable Hydrogenation. *Appl. Phys. Lett.* **2010**, *97*, 233111. [CrossRef]
5. Burgess, J.S.; Matis, B.R.; Robinson, J.T.; Bulat, F.A.; Keith Perkins, F.; Houston, B.H.; Baldwin, J.W. Tuning the Electronic Properties of Graphene by Hydrogenation in a Plasma Enhanced Chemical Vapor Deposition Reactor. *Carbon* **2011**, *49*, 4420–4426. [CrossRef]
6. Felten, A.; McManus, D.; Rice, C.; Nittler, L.; Pireaux, J.-J.; Casiraghi, C. Insight into Hydrogenation of Graphene: Effect of Hydrogen Plasma Chemistry. *Appl. Phys. Lett.* **2014**, *105*, 183104. [CrossRef]
7. Zhao, F.; Raitses, Y.; Yang, X.; Tan, A.; Tully, C.G. High Hydrogen Coverage on Graphene via Low Temperature Plasma with Applied Magnetic Field. *Carbon* **2021**, *177*, 244–251. [CrossRef]
8. Haberer, D.; Vyalikh, D.V.; Taioli, S.; Dora, B.; Farjam, M.; Fink, J.; Marchenko, D.; Pichler, T.; Ziegler, K.; Simonucci, S.; et al. Tunable Band Gap in Hydrogenated Quasi-Free-Standing Graphene. *Nano Lett.* **2010**, *10*, 3360–3366. [CrossRef] [PubMed]
9. Paris, A.; Verbitskiy, N.; Nefedov, A.; Wang, Y.; Fedorov, A.; Haberer, D.; Oehzelt, M.; Petaccia, L.; Usachov, D.; Vyalikh, D.; et al. Kinetic Isotope Effect in the Hydrogenation and Deuteration of Graphene. *Adv. Funct. Mater.* **2013**, *23*, 1628–1635. [CrossRef]
10. Ryu, S.; Han, M.Y.; Maultzsch, J.; Heinz, T.F.; Kim, P.; Steigerwald, M.L.; Brus, L.E. Reversible Basal Plane Hydrogenation of Graphene. *Nano Lett.* **2008**, *8*, 4597–4602. [CrossRef] [PubMed]
11. Balog, R.; Andersen, M.; Jørgensen, B.; Sljivancanin, Z.; Hammer, B.; Baraldi, A.; Larciprete, R.; Hofmann, P.; Hornekær, L.; Lizzit, S. Controlling Hydrogenation of Graphene on Ir(111). *ACS Nano* **2013**, *7*, 3823–3832. [CrossRef]
12. Whitener, K.E.; Lee, W.K.; Campbell, P.M.; Robinson, J.T.; Sheehan, P.E. Chemical Hydrogenation of Single-Layer Graphene Enables Completely Reversible Removal of Electrical Conductivity. *Carbon* **2014**, *72*, 348–353. [CrossRef]
13. Son, J.; Lee, S.; Kim, S.J.; Park, B.C.; Lee, H.-K.; Kim, S.; Kim, J.H.; Hong, B.H.; Hong, J. Hydrogenated Monolayer Graphene with Reversible and Tunable Wide Band Gap and Its Field-Effect Transistor. *Nat. Commun.* **2016**, *7*, 13261. [CrossRef] [PubMed]
14. Panahi, M.; Solati, N.; Kaya, S. Modifying Hydrogen Binding Strength of Graphene. *Surf. Sci.* **2019**, *679*, 24–30. [CrossRef]
15. Abdelnabi, M.M.S.; Blundo, E.; Betti, M.G.; Cavoto, G.; Placidi, E.; Polimeni, A.; Ruocco, A.; Hu, K.; Ito, Y.; Mariani, C. Towards Free-Standing Graphane: Atomic Hydrogen and Deuterium Bonding to Nano-Porous Graphene. *Nanotechnology* **2021**, *32*, 035707. [CrossRef] [PubMed]
16. Abdelnabi, M.M.S.; Izzo, C.; Blundo, E.; Betti, M.G.; Sbroscia, M.; di Bella, G.; Cavoto, G.; Polimeni, A.; García-Cortés, I.; Rucandio, I.; et al. Deuterium Adsorption on Free-Standing Graphene. *Nanomaterials* **2021**, *11*, 130. [CrossRef]
17. Betti, M.G.; Blundo, E.; de Luca, M.; Felici, M.; Frisenda, R.; Ito, Y.; Jeong, S.; Marchiani, D.; Mariani, C.; Polimeni, A.; et al. Homogeneous Spatial Distribution of Deuterium Chemisorbed on Free-Standing Graphene. *Nanomaterials* **2022**, *12*, 2613. [CrossRef]
18. Betti, M.G.; Placidi, E.; Izzo, C.; Blundo, E.; Polimeni, A.; Sbroscia, M.; Avila, J.; Dudin, P.; Hu, K.; Ito, Y.; et al. Gap Opening in Double-Sided Highly Hydrogenated Free-Standing Graphene. *Nano Lett.* **2022**, *22*, 2971–2977. [CrossRef] [PubMed]
19. Ito, Y.; Qiu, H.-J.; Fujita, T.; Tanabe, Y.; Tanigaki, K.; Chen, M. Bicontinuous Nanoporous N-Doped Graphene for the Oxygen Reduction Reaction. *Adv. Mater.* **2014**, *26*, 4145–4150. [CrossRef]
20. Tanabe, Y.; Ito, Y.; Sugawara, K.; Hojo, D.; Koshino, M.; Fujita, T.; Aida, T.; Xu, X.; Huynh, K.K.; Shimotani, H.; et al. Electric Properties of Dirac Fermions Captured into 3D Nanoporous Graphene Networks. *Adv. Mater.* **2016**, *28*, 10304–10310. [CrossRef]
21. di Bernardo, I.; Avvisati, G.; Mariani, C.; Motta, N.; Chen, C.; Avila, J.; Asensio, M.C.; Lupi, S.; Ito, Y.; Chen, M.; et al. Two-Dimensional Hallmark of Highly Interconnected Three-Dimensional Nanoporous Graphene. *ACS Omega* **2017**, *2*, 3691–3697. [CrossRef]
22. di Bernardo, I.; Avvisati, G.; Chen, C.; Avila, J.; Asensio, M.C.; Hu, K.; Ito, Y.; Hines, P.; Lipton-Duffin, J.; Rintoul, L.; et al. Topology and Doping Effects in Three-Dimensional Nanoporous Graphene. *Carbon* **2018**, *131*, 258–265. [CrossRef]
23. Tanabe, Y.; Ito, Y.; Sugawara, K.; Koshino, M.; Kimura, S.; Naito, T.; Johnson, I.; Takahashi, T.; Chen, M. Dirac Fermion Kinetics in 3D Curved Graphene. *Adv. Mater.* **2020**, *32*, 2005838. [CrossRef]
24. Betti, M.G.; Biasotti, M.; Boscá, A.; Calle, F.; Carabe-Lopez, J.; Cavoto, G.; Chang, C.; Chung, W.; Cocco, A.G.; Colijn, A.P.; et al. A Design for an Electromagnetic Filter for Precision Energy Measurements at the Tritium Endpoint. *Prog. Part. Nucl. Phys.* **2019**, *106*, 120–131. [CrossRef]
25. Gierz, I.; Petersen, J.C.; Mitrano, M.; Cacho, C.; Turcu, I.C.E.; Springate, E.; Stöhr, A.; Köhler, A.; Starke, U.; Cavalleri, A. Snapshots of Non-Equilibrium Dirac Carrier Distributions in Graphene. *Nat. Mater.* **2013**, *12*, 1119–1124. [CrossRef] [PubMed]

26. Wang, H.; Strait, J.H.; George, P.A.; Shivaraman, S.; Shields, V.B.; Chandrashekhar, M.; Hwang, J.; Rana, F.; Spencer, M.G.; Ruiz-Vargas, C.S.; et al. Ultrafast Relaxation Dynamics of Hot Optical Phonons in Graphene. *Appl. Phys. Lett.* **2010**, *96*, 081917. [CrossRef]
27. Ulstrup, S.; Christian Johannsen, J.; Crepaldi, A.; Cilento, F.; Zacchigna, M.; Cacho, C.; Chapman, R.T.; Springate, E.; Fromm, F.; Raidel, C.; et al. Ultrafast Electron Dynamics in Epitaxial Graphene Investigated with Time- and Angle-Resolved Photoemission Spectroscopy. *J. Phys. Condens. Matter* **2015**, *27*, 164206. [CrossRef]
28. Xu, Y.; Wang, R.; Ma, S.; Zhou, L.; Shen, Y.R.; Tian, C. Theoretical Analysis and Simulation of Pulsed Laser Heating at Interface. *J. Appl. Phys.* **2018**, *123*, 025301. [CrossRef]
29. Nair, R.R.; Blake, P.; Grigorenko, A.N.; Novoselov, K.S.; Booth, T.J.; Stauber, T.; Peres, N.M.R.; Geim, A.K. Fine Structure Constant Defines Visual Transparency of Graphene. *Science (1979)* **2008**, *320*, 1308. [CrossRef]
30. Chien, S.-K.; Yang, Y.-T.; Chen, C.-K. Influence of Hydrogen Functionalization on Thermal Conductivity of Graphene: Nonequilibrium Molecular Dynamics Simulations. *Appl. Phys. Lett.* **2011**, *98*, 033107. [CrossRef]
31. Mortazavi, B.; Madjet, M.E.; Shahrokhi, M.; Ahzi, S.; Zhuang, X.; Rabczuk, T. Nanoporous Graphene: A 2D Semiconductor with Anisotropic Mechanical, Optical and Thermal Conduction Properties. *Carbon* **2019**, *147*, 377–384. [CrossRef]
32. Song, B.; Gu, H.; Zhu, S.; Jiang, H.; Chen, X.; Zhang, C.; Liu, S. Broadband Optical Properties of Graphene and HOPG Investigated by Spectroscopic Mueller Matrix Ellipsometry. *Appl. Surf. Sci.* **2018**, *439*, 1079–1087. [CrossRef]
33. Neek-Amal, M.; Peeters, F.M. Lattice Thermal Properties of Graphane: Thermal Contraction, Roughness, and Heat Capacity. *Phys. Rev. B* **2011**, *83*, 235437. [CrossRef]
34. Kashani, H.; Ito, Y.; Han, J.; Liu, P.; Chen, M. Extraordinary Tensile Strength and Ductility of Scalable Nanoporous Graphene. *Sci. Adv.* **2019**, *5*, eaat6951. [CrossRef] [PubMed]
35. Zhang, H.; Miyamoto, Y.; Rubio, A. Laser-Induced Preferential Dehydrogenation of Graphane. *Phys. Rev. B* **2012**, *85*, 201409. [CrossRef]
36. Curcio, D.; Pakdel, S.; Volckaert, K.; Miwa, J.A.; Ulstrup, S.; Lanatà, N.; Bianchi, M.; Kutnyakhov, D.; Pressacco, F.; Brenner, G.; et al. Ultrafast Electronic Linewidth Broadening in the C 1s Core Level of Graphene. *Phys. Rev. B* **2021**, *104*, L161104. [CrossRef]
37. Pozzo, M.; Alfè, D.; Lacovig, P.; Hofmann, P.; Lizzit, S.; Baraldi, A. Thermal Expansion of Supported and Freestanding Graphene: Lattice Constant versus Interatomic Distance. *Phys. Rev. Lett.* **2011**, *106*, 135501. [CrossRef]
38. Ferrari, E.; Galli, L.; Miniussi, E.; Morri, M.; Panighel, M.; Ricci, M.; Lacovig, P.; Lizzit, S.; Baraldi, A. Layer-Dependent Debye Temperature and Thermal Expansion of Ru(0001) by Means of High-Energy Resolution Core-Level Photoelectron Spectroscopy. *Phys. Rev. B* **2010**, *82*, 195420. [CrossRef]
39. Ito, Y.; Cong, W.; Fujita, T.; Tang, Z.; Chen, M. High Catalytic Activity of Nitrogen and Sulfur Co-Doped Nanoporous Graphene in the Hydrogen Evolution Reaction. *Angew. Chem. Int. Ed.* **2015**, *54*, 2131–2136. [CrossRef]
40. Ito, Y.; Tanabe, Y.; Han, J.; Fujita, T.; Tanigaki, K.; Chen, M. Multifunctional Porous Graphene for High-Efficiency Steam Generation by Heat Localization. *Adv. Mater.* **2015**, *27*, 4302–4307. [CrossRef] [PubMed]
41. Ito, Y.; Tanabe, Y.; Qiu, H.-J.; Sugawara, K.; Heguri, S.; Tu, N.H.; Huynh, K.K.; Fujita, T.; Takahashi, T.; Tanigaki, K.; et al. High-Quality Three-Dimensional Nanoporous Graphene. *Angew. Chem. Int. Ed.* **2014**, *53*, 4822–4826. [CrossRef] [PubMed]
42. Hu, K.; Qin, L.; Zhang, S.; Zheng, J.; Sun, J.; Ito, Y.; Wu, Y. Building a Reactive Armor Using S-Doped Graphene for Protecting Potassium Metal Anodes from Oxygen Crossover in K–O 2 Batteries. *ACS Energy Lett.* **2020**, *5*, 1788–1793. [CrossRef]
43. Bischler, U.; Bertel, E. Simple Source of Atomic Hydrogen for Ultrahigh Vacuum Applications. *J. Vac. Sci. Technol. A Vac. Surf. Film.* **1993**, *11*, 458–460. [CrossRef]
44. Costantini, R.; Stredansky, M.; Cvetko, D.; Kladnik, G.; Verdini, A.; Sigalotti, P.; Cilento, F.; Salvador, F.; de Luisa, A.; Benedetti, D.; et al. ANCHOR-SUNDYN: A Novel Endstation for Time Resolved Spectroscopy at the ALOISA Beamline. *J. Electron Spectros. Relat. Phenom.* **2018**, *229*, 7–12. [CrossRef]
45. Costantini, R.; Cilento, F.; Salvador, F.; Morgante, A.; Giorgi, G.; Palummo, M.; Dell'Angela, M. Photo-Induced Lattice Distortion in 2H-MoTe 2 Probed by Time-Resolved Core Level Photoemission. *Faraday Discuss.* **2022**, *236*, 429–441. [CrossRef] [PubMed]
46. Costantini, R.; Faber, R.; Cossaro, A.; Floreano, L.; Verdini, A.; Hättig, C.; Morgante, A.; Coriani, S.; Dell'Angela, M. Picosecond Timescale Tracking of Pentacene Triplet Excitons with Chemical Sensitivity. *Commun. Phys.* **2019**, *2*, 56. [CrossRef]